Fusion Engineering and Design 154 (2020) 111512

Contents lists available at ScienceDirect

Fusion Engineering and Design

journal homepage: www.elsevier.com/locate/fusengdes

2-D moving mesh modeling of lithium dryout in open surface liquid metal flow applications

M. Szott*, D.N. Ruzic

Department of Nuclear, Plasma and Radiological Engineering, University of Illinois, Urbana, IL 61801, United States

ARTICLE INFO

Keywords:
Liquid lithium
Dryout
Plasma facing component
Thermoelectric magnetohydrodynamics
COMSOL Multiphysics
Moving mesh

ABSTRACT

Liquid lithium displays increasing promise as a replacement for solid plasma facing components (PFCs) in fusion device applications. The Liquid Metal Infused Trench (LiMIT) system, developed at the University of Illinois (UIUC), has demonstrated how thermoelectric magnetohydrodynamics (TEMHD) can be harnessed to drive liquid lithium flow in an open surface PFC. However, in the highest heat flux applications, large local acceleration is created via TEMHD, and the sudden increase in velocity can cause the liquid level to expose the underlying solid, eliminating the protective benefits of the lithium. In order to study potential mitigation strategies, a 2-D COMSOL Multiphysics model was developed using the moving mesh module to capture free surface flow. The model depicts the development of the dryout phenomenon for 2 test cases – slow (1 cm/s) and medium (10 cm/s) flow in 5 mm deep trenches – including the liquid level reduction under the high heat flux and the pileup of slower flow both upstream and downstream of the heat stripe. The effectiveness of trench shaping dryout mitigation strategies is examined. For the slow flow case, it is shown that a 1.8 mm ledge placed under the heat stripe will stop dryout, and for the medium flow case, a 2.7 mm ledge is required to mitigate the effect. This model can be used to identify strategies for increasing the viable heat load for open surface liquid lithium PFCs.

1. Introduction

As the development of confined fusion systems progresses, plasma facing components (PFCs) must withstand ever increasing heat and particle fluxes and contend with disruptions. Wall materials must deal with the high heat load and irradiation without failing. In these high intensity conditions, solid materials struggle to cope, sustaining erosion [1–3], thermal damage [4], and fuzz formation [5,6]. Since these solid wall materials are generally of high atomic number (high-Z), damage to the wall induces strong negative feedback to plasma parameters as well. To combat these issues, increasing focus has been given to liquid metal PFCs, specifically liquid lithium. Lithium is low-Z, and if it enters the plasma through sputtering or evaporation it will cause minimal losses on core plasma performance [7]. Significant benefits of the use of lithium have been seen in tokamaks and stellarators (TFTR, FTU, CDX-U, NSTX, LTX, DIII-D, TJ-II, etc.), including low recycling of impurities and exhaust products from the wall, increased confinement time, increased and more stable density and temperature profiles, and even disruption mitigation [8–18].

Flowing liquid lithium surfaces can alleviate the issues solid PFCs face by presenting a constantly refreshing liquid surface that is immune to damage and passivation, reduces erosion of high-Z materials, and improves heat transfer while protecting the solid surfaces beneath. Two of the main open surface liquid lithium flow technologies are the FLiLi system, developed at PPPL, and the Liquid Metal Infused Trench (LiMIT) system, developed at the University of Illinois (UIUC) [19]. The FLiLi concept consists of a thin film of lithium that falls down a smooth plate. Lithium is pumped to the top of the device and pushed through a distributor nozzle, a series of small holes meant to disperse the flow into a thin film. The plate is cooled from beneath, allowing the temperature of the lithium to stay in a low evaporation regime. Designs of this concept were developed for placement on the HT-7 and EAST tokamaks [20–22]. LiMIT has demonstrated controlled open surface liquid lithium flow driven through solid trenches by harnessing the thermoelectric magnetohydrodynamic (TEMHD) effect [23,24]. The concept has been successfully tested at UIUC [25–27] and in systems around the world, including the HT-7 tokamak [28,29], and the Magnum PSI linear plasma device [30], at sustained heat fluxes up to 3 MW/m^2. During sustained heat flux above this point, or transient heat loads > 10 MW/m^2, the phenomenon of lithium dryout could occur.

The term dryout is commonly used to describe the phenomenon that occurs as a liquid reaches its critical heat flux and begins to exhibit film boiling [31]. The type of dryout investigated here, however, is relatively limited in its relevance, and no free surface liquid lithium

* Corresponding author.
E-mail address: szott1@illinois.edu (M. Szott).

https://doi.org/10.1016/j.fusengdes.2020.111512
Received 3 September 2019; Received in revised form 27 January 2020; Accepted 27 January 2020

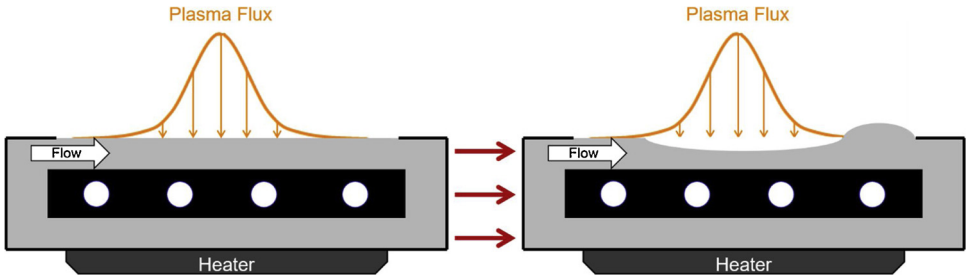

Fig. 1. A diagram of the lithium dryout phenomenon in a TEMHD-driven flowing liquid lithium system. When high local heat flux impacts a flowing lithium surface, local acceleration causes a depression of the lithium surface and pileup both upstream and downstream.

technology has progressed far enough to warrant further scrutiny into this effect. As plasma flux impinges on the open surface of the lithium flow, the lithium experiences a high local acceleration where the plasma flux is greatest. This change in flow conditions leads to a depression of the lithium surface and pileup of the lithium downstream. This is depicted in the diagrams in Fig. 1. When the lithium surface depresses to the point of exposing underlying solid material, lithium dryout occurs.

Dryout in a liquid PFC system can be severely damaging, especially in a LiMIT-type trench array. As the lithium level decreases, the tops of the trenches may become exposed. If this occurs, the solid metal is now directly impacted by the plasma, which could lead to overheating and the exact damage a liquid metal system is built to avoid. Depending on flow conditions, a negative feedback may develop, with the thinner lithium surface moving faster but now absorbing the same heat flux as with a fully filled trench, leading to higher heat flux passthrough to the solid surfaces.

One prime example is in tests of the LiMIT apparatus at UIUC [32]. In this case, a homemade electron beam system provides the heat flux, and a set of external electromagnetic coils provide the transverse magnetic field. As the e-beam is activated, a strong heat flux impinges on the lithium surface and begins driving flow.

In the beginning of the video from which the images in Fig. 2 are pulled, lithium sits stationary slightly under the level of the trenches. This is the static case shown in the left image. While this test begins in an underfilled scenario (lithium level starts below the level of the trenches), the characteristic behaviors of lithium dryout conditions are seen. As the flow begins, lithium velocity increases in the e-beam strikepoint region and lithium buildup occurs downstream. The right image shows the LiMIT module shortly after flow begins and includes the 2–3 mm buildup from the high velocity lithium exiting the e-beam region, small waves in the e-beam region from the accelerating flow, and ~1 mm increase in upstream lithium height. As the video progresses, the pileup is drained out from the downstream region through the return flow channels. The 1–1.5 mm lithium depression formed in the high heat flux region persists through the video and high velocity flow continues downstream of the impingement area.

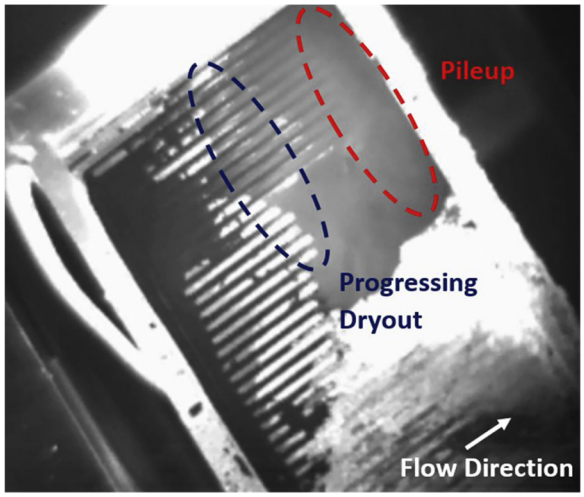

Fig. 3. Infrared camera image of dryout beginning during LiMIT testing at the Magnum PSI linear plasma device. Trenches progressively become more visible as they heat up due to the lithium level reduction. Note that there is still lithium coverage throughout a majority of the device, though it is being reduced in the indicated region. Though some trenches appear uncovered, this is due to the differences in emissivity between lithium, stainless steel, and surface impurities.

Another example of dryout observed in experimental testing occurred in LiMIT tests under high heat loads at Magnum-PSI [30]. Due to the larger heat flux spread from the linear plasma device, an apt comparison is not as direct. However, lithium dryout and pileup are still seen qualitatively in the image in Fig. 3. The infrared snapshot from a video of one of the Magnum PSI tests of the LiMIT module shows trenches becoming more visible as lithium thins above them and they receive more heat from the plasma. The trenches become visible from the top left to the bottom right of the 'Progressing Dryout' region as the

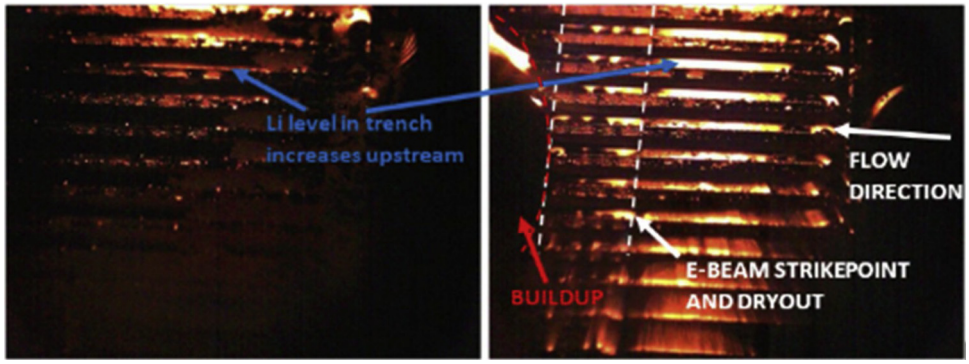

Fig. 2. Experimental observation of lithium dryout in LiMIT testing at UIUC. The left frame shows the stationary case before the electron beam heat flux instigates dryout and pileup, as seen in the right frame.

test progresses. Due to small recirculation channels in this version of the LiMIT apparatus, pileup occurs downstream, but does not drain as in the test in Fig. 2. This is indicated by the disappearance of the trenches in the 'Pileup' region of the IR image.

There are several potential mitigation strategies for liquid lithium dryout, including trench shaping, partial trench removal, and addition of a constraining mesh. Trench shaping entails narrowing the height of the trenches in regions of high plasma heat flux in order to compensate for the increased velocity. Another option is allowing and planning for the plasma depression of the lithium. In this case, the trench walls are reduced in height to follow the depression level, keeping them submerged in the liquid lithium. Since this depression will cause pileup downstream, it would be wise to allow a larger outlet to accommodate and alleviate the lithium pileup. Finally, a third option is the addition of a thin mesh to the tops of the trenches. Lithium has a very high surface tension, so this mesh could constrain the surface of the lithium without impeding bulk flow. The mesh may not be well protected, however, as only a thin film will cover the wiring (especially in the highest heat flux regions), so the mesh may degrade over time and need replacement. This is still a more desirable outcome than damage to the bulk solid first wall components. Illustrations of these options are shown in Fig. 4.

Until this point, computational studies [26] of the flowing liquid lithium in the LiMIT system have consistently constrained the lithium in a rigid domain. While this may be fully accurate if the liquid is truly constrained, such as in pipe flow, the solution lacks completeness when an open surface exists. Fluids slosh around when forces act upon them, and this behavior cannot be captured when a rigid domain is used. The usual solution is to make the top surface a slip boundary condition, which mimics an open surface by eliminating the frictional force from the walls. This treatment is generally effective in describing flow conditions, and has been used to model and predict flow velocities in LiMIT trenches [26]. However, the shape of some velocity profiles in constrained surface flow models imply a dryout condition would occur.

To that end, COMSOL Multiphysics was used here to develop a 2-D simulation of free surface lithium flow under high heat flux, with the goal of replicating the dryout phenomenon and taking steps to alleviate it.

2. Theory and domain setup

The simulation is performed in a 2-D simplified domain in COMSOL v4.3. In order to reduce computational constraints, a 2-D slice of a 3-D trench is modeled in the domain shown in Fig. 5. Previous modeling of TEMHD flow in the LiMIT system relied on a fixed topside lithium boundary that approximated an open surface by including a slip boundary condition. In order to accurately capture the behavior of the free surface, this model simplifies the system to 2-D and couples the Laminar Flow (LF) module with the Moving Mesh (MM) module.

For the two test cases presented here, 1 cm/s and 10 cm/s flow, the Reynolds number is 50 and 500, respectively, allowing the laminar flow interface to be used. Assuming a steady state flow case with low 500 K/m temperature gradient before a topside heat flux is introduced, this corresponds to a magnetic field of 1 T and 0.05 T. The Single Phase Flow, Laminar Flow physics interface solves the Navier-Stokes continuity and momentum equations to find the pressure and velocity field of the liquid [33]. Assuming incompressibility, these equations become

$$\rho\nabla\cdot\boldsymbol{u} = 0$$

$$\rho\frac{\partial \boldsymbol{u}}{\partial t} + \rho(\boldsymbol{u}\cdot\nabla)\boldsymbol{u} = \nabla\cdot[-p\boldsymbol{I} + \mu(\nabla\boldsymbol{u} + (\nabla\boldsymbol{u})^T)] + \boldsymbol{F}$$

Where ρ is the density, $\boldsymbol{u}$ is the velocity vector, p is the pressure, $\boldsymbol{I}$ is the identity matrix, μ is the dynamic viscosity, and $\boldsymbol{F}$ is the force vector. The inlet and outlet are included using zero pressure boundary conditions with suppressed backflow. An attempt was made to link the inlet and outlet using a periodic flow condition, but the dryout deformation passing from the outlet to the inlet side of the domain caused errors to amass and the solution to diverge. The top surface is a free surface modeled as an open boundary with 0 normal stresses on the surface. The bottom surface is a no slip boundary condition.

The development of the thermoelectric current is dependent on the junction between the lithium and a wall, and inherently 3-dimensional (looping into and out of the page in the domain view), and therefore the full coupling between heat transfer, magnetic field, and electric currents cannot be included via modules in this model. Instead, a Gaussian volume force term is included in the LF module that takes the entirety of the TEMHD effect into account. In a 3-D domain, a Gaussian heat flux leads to a thermoelectric current, which in turn is used to calculate a volume force. In COMSOL post-processing, the volume force data was examined. The vertical volume force is a combination of the velocity and fluid effects, as well as the errant thermal gradient effects. From 3-D simulations, the volume force data was extracted and input into this 2-D domain, in the form

$$F = F_{max}\exp\left(\frac{-(x - x_{centerpoint})^2}{FWHM^2}\right)\left[N/m^3\right]$$

The F_{max} value for the slow 1 cm/s flow case is set at 10 N/m^3, mimicking a 1 MW/m^2 peak heat flux, while the F_{max} for the medium flow 10 cm/s case is set to 1000 N/m^3, indicative of a 3 MW/m^2 peak heat flux. These values are based on 3-D fixed surface models of a LiMIT trench.

The important improvement in this work is the addition of the moving mesh. The interface allows the free surface to deform in response to the fluid flow on the top surface. This allows the mesh movement to be coupled with the driving force provided by the TEMHD effect. Typically, physical systems are set up and solved computationally in one of two coordinate systems. The spatial coordinate system, known as the Eulerian formulation, fixes the coordinate axes in space, and the material coordinate system, known as the Lagrangian formulation, fixes the coordinates to the reference material and follows the material as it deforms. For fluid solutions, the Eulerian formulation tends to be more convenient, since following the particles becomes quite computationally intensive. However, since the grid points are fixed to a spatial system, an Eulerian method cannot follow moving domain boundaries, which are a staple in open surface flow. One way to get around this problem is to use a convenient feature that is always included in COMSOL – the mesh. The mesh points created in COMSOL have a direct mapping to material domain points. Therefore, if the mesh were to deform and follow the mobile domain, it is possible to use an Eulerian mapping to solve for a deforming Lagrangian-type system. This is known as an arbitrary Lagrangian-Eulerian process, and it is included as the solver in the MM module [33]. As the domain deforms, the mesh is stretched and compressed along with the domain motion. While this

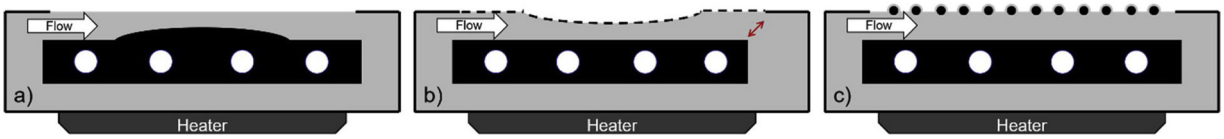

Fig. 4. Initial concepts for dryout mitigation. a) 'Trench shaping' increases the lithium level by adjusting the bottom of the trench. b) 'Trench removal' plans for dryout and removes portions of the trench walls in the highest heat flux areas, while increasing the outlet size for improved drainage. c) 'Mesh inclusion' is meant to constrain the free surface while allowing underlying flow, utilizing the high surface tension of lithium.

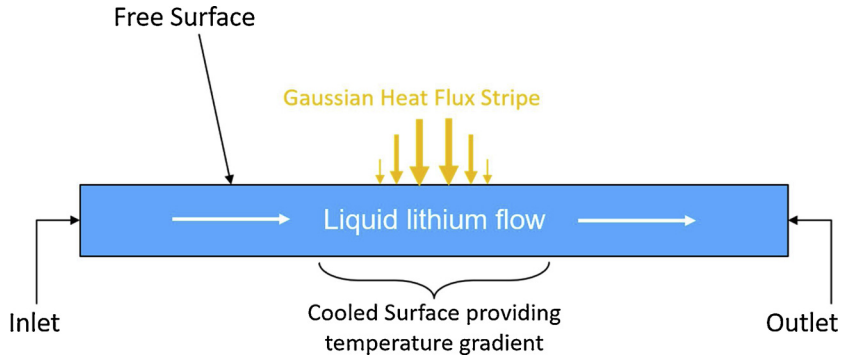

Fig. 5. 2-D COMSOL domain used to simulate the dryout phenomenon. The top surface is modeled as a free surface and the Moving Mesh module allows deformation to follow liquid motion.

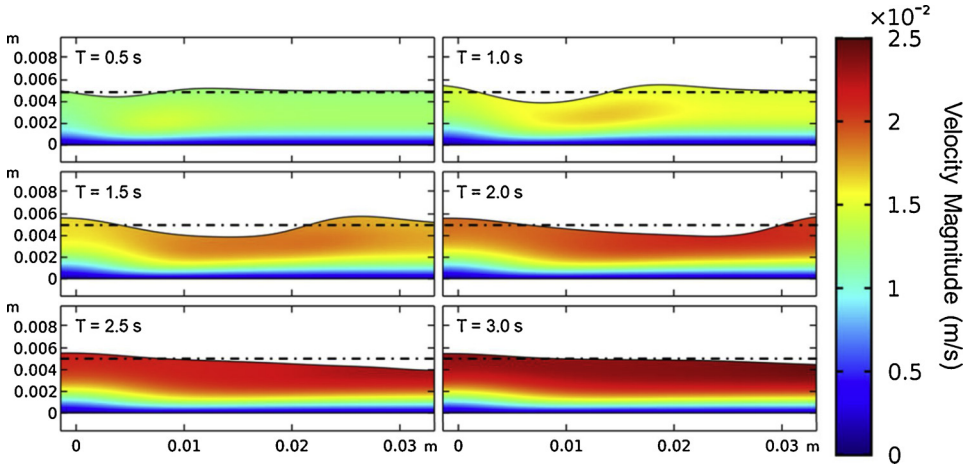

Fig. 6. Frame-by-frame (every 0.5 s) results of slow flow dryout development. Initial velocity is 1 cm/s. The color map shows flow velocity, and the dotted line marks the trench level/nominal lithium level.

deformation can cause degradation of the mesh quality that can lead to a buildup of solver error, small disturbances can be effectively solved with a fine enough mesh.

Implementation of the MM module requires choosing what boundaries and domains are allowed to deform, and in what way. For this system, there is only one domain, which is allowed free deformation. In order to constrain that deformation, and hold it in its trench shape, prescribed displacements are used on the edges. The bottom surface is a no slip surface that has a prescribed displacement of 0 m in both the horizontal and vertical directions. This keeps the bottom fixed at all times. The inlet and outlet edges on the sides of the domain have a prescribed displacement of 0 m in the horizontal direction, and no constraint vertically. This allows the edges to follow any vertical motion in the domain, such as dryout or pileup, while still acting as a fixed inlet or outlet. The free surface on the top, meanwhile, is modeled using a prescribed mesh velocity. Velocities solved by the laminar flow module are coupled with this step, and the mesh deforms to match the true behavior of the fluid in the horizontal and vertical directions.

Using the arbitrary Lagrangian-Eulerian system to solve for a variable v, COMSOL defines a frame time derivative on the spatial frame, and a mesh time derivative on the fixed mesh points

$$v_t(x_0, y_0) = \left.\frac{\partial v}{\partial t}\right|_{x_0,y_0}$$

$$v_{TIME}(X_m, Y_m) = \left.\frac{\partial v}{\partial t}\right|_{X_m,Y_m}$$

And relates them using

$$v_t = v_{TIME} - v_x x_{TIME} - v_y y_{TIME}$$

Where (x_{TIME}, y_{TIME}) is the mesh velocity. Within deforming domains, a mesh displacement equation is solved to determine how the region deforms. A Winslow smoothing algorithm is chosen to deform the mesh, which leads the software to solve

$$\frac{\partial^2 X}{\partial x^2} + \frac{\partial^2 X}{\partial y^2} = 0 \, and \, \frac{\partial^2 Y}{\partial x^2} + \frac{\partial^2 Y}{\partial y^2} = 0$$

Here X and Y are the material frame coordinates, and x and y are the coordinates of the spatial frame [33]. Solutions in 2-D require less memory, so a MUMPS direct solver is used to solve the fully coupled system.

3. Model results

The model was run for up to 3 s after heat flux impingement begins. Two separate cases were examined, a slow flow case with 1 cm/s velocity, and a fast flow case where the velocity is 10 cm/s. These can be thought of as low heat flux and high heat flux cases, as the volume force is adjusted accordingly based on the amount of flux the flow speed can handle. The system is initialized with aforementioned velocities, as though lithium flow was established using an alternative heat flux, such as heaters on the bottom of the trench. The impingement heat flux is centered at 0 cm in the domain and starts at t = 0 s.

The slow flow case is shown in the series of images in Fig. 6. Again, the color map represents lithium velocity. As the simulation begins, the dryout begins to form in the center, directly under the highest heat flux. This is due to the preferential heating of the lithium in the depressed region, which is then accelerated by the large thermal gradient resulting from passing through the heat stripe. The dryout is then

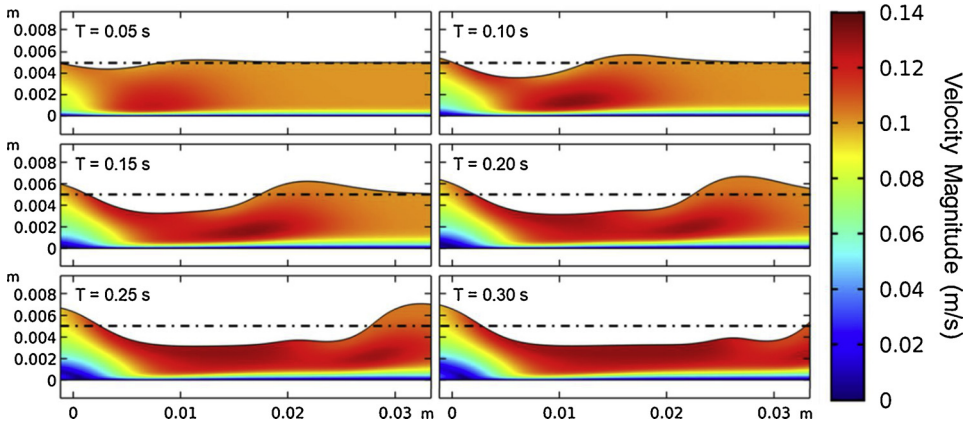

Fig. 7. Frame-by-frame results (every 0.05 s) of fast flow dryout development. Initial velocity is 10 cm/s. The color map shows flow velocity, and the dotted line marks the trench level/nominal lithium level.

propelled down the trench by the flow. Lithium pileup occurs downstream of the high heat flux region, as high velocity lithium accelerates into slower downstream flow. As this reaches the end of the trench, spillover could occur, damaging other components that are not necessarily compatible with the hot liquid lithium. It is also interesting that as the dryout forms, there is upstream buildup that occurs during its transient development. This is due to lithium building up against the reduced cross-sectional area of the flow before accelerating through the high heat flux region. Additionally, as the initial heat flux impact depresses the lithium surface, the pressure from that quick acceleration actually extends in both directions. This causes upwelling on either side of the depression like when a rock impacts shallow water and the entire area around it wells up before splashing. This effect starts the upwelling, and the continuation of flow into these regions helps maintain the pileup.

The fast flow case exhibits the same behavior, albeit faster than the slow flow tests. The set of images describing this case is given in Fig. 7. Dryout forms under the heat flux region and extends downstream. The pileup quickly moves toward the end of the trench, and eventually leaves the domain, meaning half of the length of the trenches are potentially exposed. Note any lithium level below the initialized 5 mm will expose trench material.

These models directly mimic what has been observed in experimental testing. While the tests shown above were not originally set up to measure dryout, so the video quality is not conducive to quantifying the exact height, the 1–3 mm buildup in the model is very similar to what is seen in experiment. Lithium depression on the order of 1–2 mm also matches the experimental cases. The domain setup in this case more closely mirrors the LiMIT setup at UIUC, where there is ample drainage for the initial downstream pileup and the dryout propagates downstream from the high heat flux region with some rippling effects due to the initial impulse. The model also shows the upstream upwelling seen in the LiMIT testing.

4. Model extension

While an exact experimental comparison may not be possible due to the 2D nature of the model and the simplifications it requires, the behavior captured in this model provides a starting point for engineering decisions regarding a solution to the dryout problem. Of the potential mitigation strategies described above, perhaps the most straightforward is shaping the bottom of the trenches, either by machining or inserting additional material into the bottoms of the trenches. This method is also testable in the COMSOL model. The effect of trench insert shapes can be investigated before real world application. This allows for quick iteration through possible designs. Several different strategies were tested, and while they may have provided a solution to the dryout, in most cases the eventual return to original trench depth caused a small waterfall-like depression in the lithium surface. This may be acceptable since the depression occurs outside of the high heat flux area, but for now that effect was avoided.

It seems as though what may be one of the simplest ideas could actually become one of the best solutions to the dryout effect. A simple step increase in the height of the bottom of the trench provided multiple benefits in both the slow and fast flow cases. First, the extended region of the narrowed trench height directly combated the extended region of the dryout by compensating for the depression caused by the high velocity flow. Second, the slight offset from center allowed the buildup that generally occurs in front of underwater flow obstructions to be placed directly underneath the area of strongest heat flux. The initial strong depression of the surface is directly opposed by this upwelling from the trench step. This can actually provide additional thermal protection of the underlying solid trenches. Third, the height of the pileup above the dryout is diminished. In other words, deviations from an average flow height are decreased. Instead the bulk flow from the center of the trench continuing downstream is raised slightly, which will not severely impact flow velocity and will also provide more protection for the trenches.

The strength of the above effects varies based on the magnitude of the trench-bottom height increase. This was investigated with the COMSOL model by running a parametric sweep over the height of the step increase. The height was varied from 0.3 mm to 3 mm (initial depth is 5 mm) with a step of 0.3 mm, and various metrics of the flow properties were extracted for each parametric solution. These parameters of the flow are diagramed in Fig. 8 for clarity.

The results of the parametric analysis are presented in Fig. 9 for the slow flow and the fast flow scenarios. First, it is worth noting that the trends plotted above for the slow flow case terminate at a step size of 2.1 mm. At heights greater than 2.1 mm, the dryout minimum fully disappears, and the upwelling caused by the trench step just pushes downstream into the small initial downstream pileup. At this point, the ledge effect causes lithium to rise several millimeters above the initial level, so these heights are discounted. As expected, increasing the ledge in the bottom of the trench helps to decrease the minimum lithium level. By a height of 1.5 mm, the minimum is above the level of the 5 mm trench, meaning dryout would be avoided. One can also see that while the pileup slightly increases, the difference between the maximum and minimum lithium level continues to drop as ledge height increases. While the ledge effect pileup keeps increasing, for a 2.1 mm ledge the lithium height is still within 3 mm of the trench, which should provide good protection for the trenches in the high heat flux region without causing too much turbulence. After consideration of the trends, 1.8 mm seems to be an ideal height for the trench ledge. At this height, there is a very small difference between the maximum and minimum

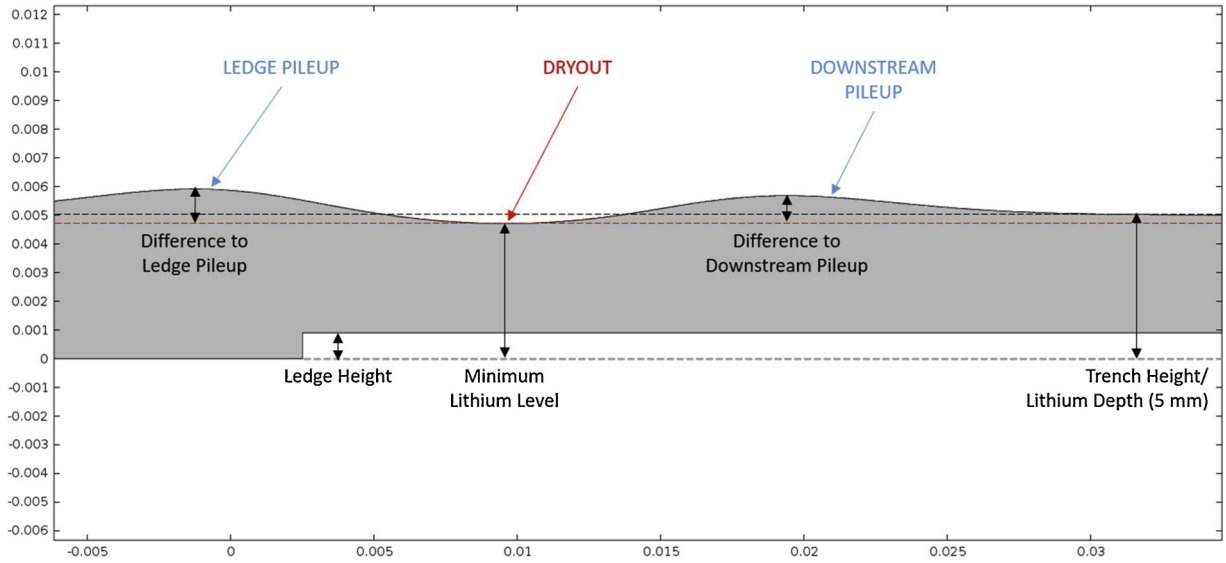

Fig. 8. Diagram of different flow metrics measured during testing of trench shaping dryout mitigation techniques in the COMSOL model.

lithium levels at both time of minimum and time of maximum. The ledge and downstream pileups are limited, while ensuring the dryout minimum stays above the level of the trenches. In all of the cases, the recirculation zone or drain area should be expanded to account for inevitable lithium pileup. However, instead of being a single wave, the lithium level will be relatively sustained. To further illustrate the ledge effects, the series in Fig. 10 shows the comparison between step sizes using the same time step for each of the tested ledge heights, up to 2.1 mm, and Fig. 11 gives an example of how the flow develops in time for one of those ledge heights (1.8 mm).

For the fast flow case, the high velocity makes for a more turbulent scenario. High ledge effect lithium levels are unavoidable, but again, this helps to protect the trenches facing the largest heat fluxes. It takes at least a 2.4 mm step increase in the height of the bottom of the trench to fully counteract the effect of dryout. This is expected, since the higher heat flux and faster velocity should combine to create a stronger dryout scenario. In this fast flow case, the maximum pileup actually tends to decrease slightly as ledge height is increased. While the ledge effect lithium level keeps increasing, it does not adversely affect the drainage like the downstream pileup would, so it is decided that a ledge height of 2.7–3.0 mm would work for a high heat flux, high velocity case. These heights maximize dryout alleviation and minimize

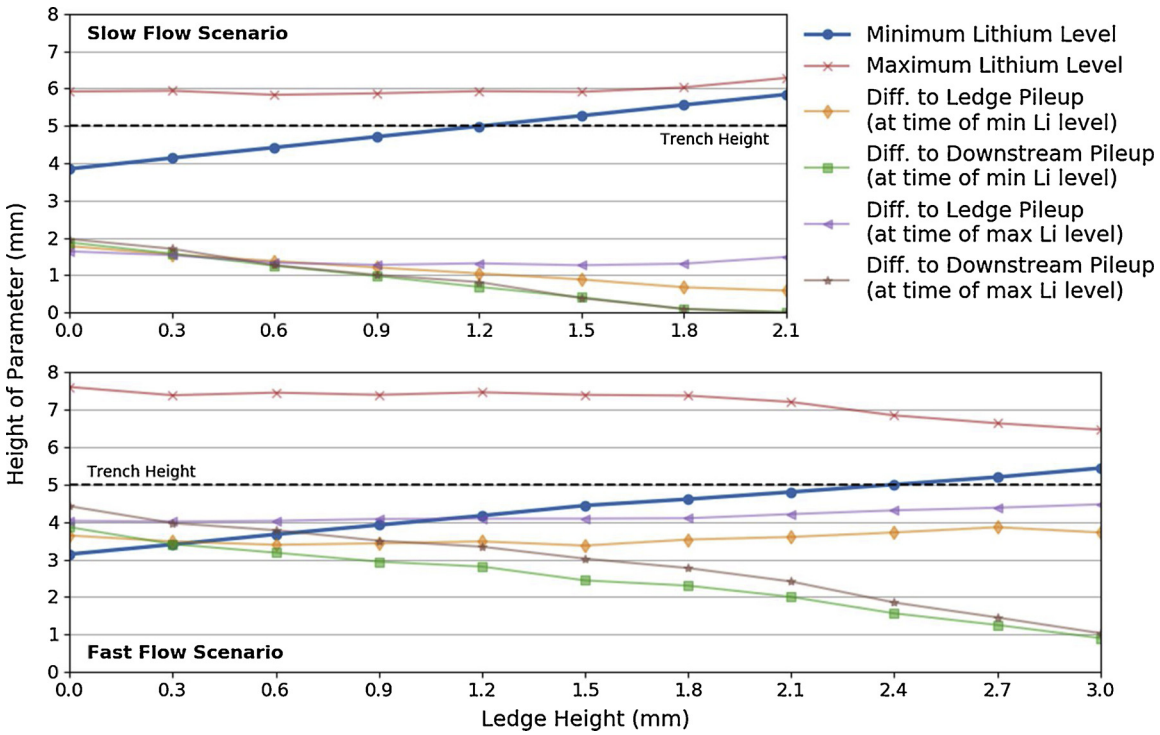

Fig. 9. Change of various dryout-relevant metrics measured from the parametric COMSOL study of increasing ledge height bottom in the bottom of the trench. Refer to Fig. 8 for a diagram of the metrics plotted. Minimum lithium level is the most important measure of dryout, as the lithium must stay above the solid trench material. The maximum lithium level indicates the highest levels of pileup – this should be kept low to minimize risk of droplet ejection. The remaining values represent the peak to peak differences in lithium level when dryout is most severe (min Li level) and when pileup is most pronounced (max Li level).

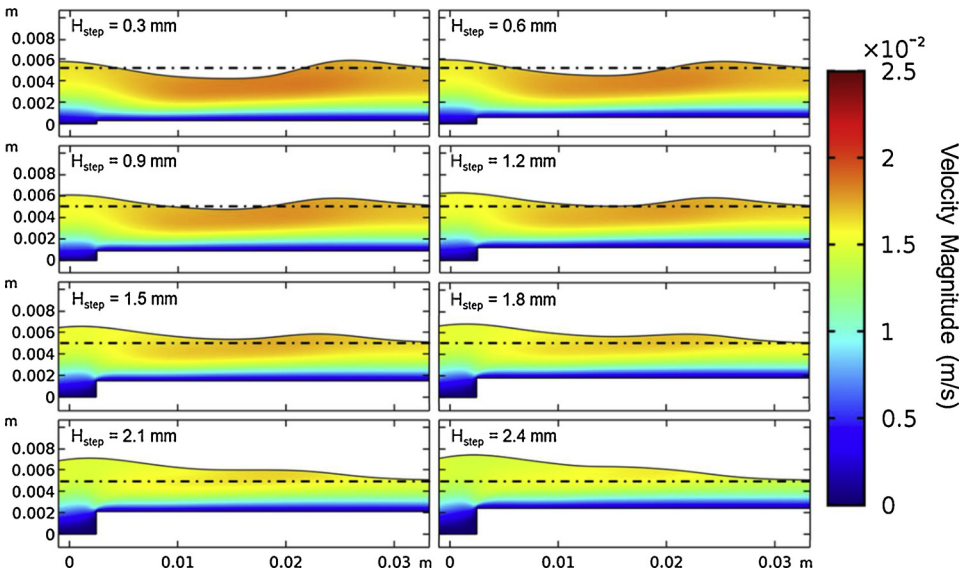

Fig. 10. The same time step (1.5 s) presented for differing trench ledge heights, showing the mitigating effect trench shaping has on development of dryout. The color map shows flow velocity (initial 1 cm/s velocity), and the dotted line marks the trench level/nominal lithium level. Refer to Fig. 6 for a reference dryout case with no trench shaping.

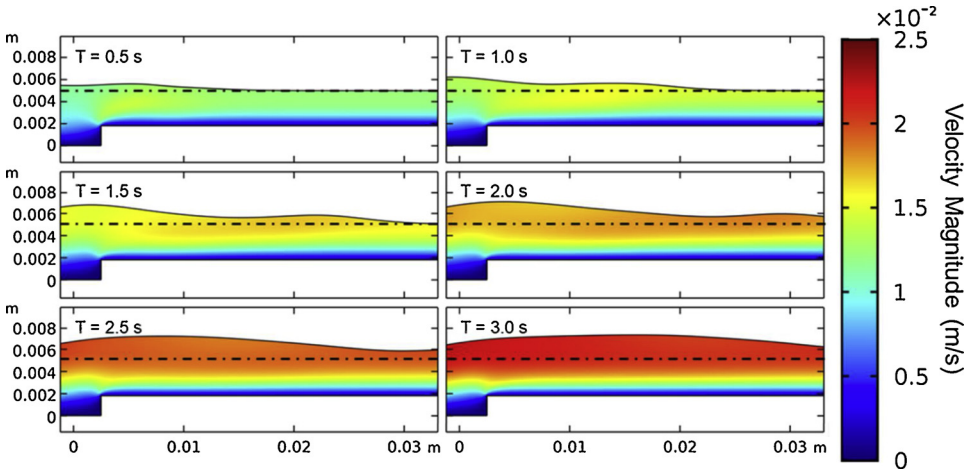

Fig. 11. Frame-by-frame (every 0.5 s) of the best case for slow flow dryout mitigation using trench shaping (1.8 mm insert). The color map shows flow velocity (1 cm/s initial velocity), and the dotted line marks the trench level/nominal lithium level.

downstream pileup.

5. Discussion and application

Maintaining a steady flowing liquid surface in the face of extreme heat fluxes is imperative for continued application of flowing liquid lithium PFCs. Testing in high heat flux environments such as the e-beam at UIUC, the divertor region in HT-7, or the linear plasma in Magnum-PSI has led to trench exposure as the lithium surface is depressed. Downstream pileup due the dryout formation and inadequate drainage for recirculation has also been observed. The model presented here accurately depicts these experimental observations using the Moving Mesh module in COMSOL Multiphysics to model true free surface flow. The mesh can deform in response to the volume forces present, instead of staying locked in a rigid domain. While currently limited to a 2-D slice of a trench system, the model still provides a valid engineering basis for further development of dryout mitigation strategies. Trench shaping can be directly implemented, as seen in the model extension above. Trench removal ideas can also be incorporated by adapting the rigid 3-D models and importing volume force profiles to investigate how the free surface will react.

There are several phenomena the model does not take into account, which can have varying relevance depending on system conditions. As mentioned, the full physics coupling of heat transfer and electric currents is not included due to inherent 3-D effects. Surface tension is not included in the motion of the free surface, as the single-phase moving mesh coupling does not utilize a true interface between a liquid and a gas/vacuum. This also means evaporation or surface transport is not included. However, in standard LiMIT experimental conditions, the temperature of the lithium is designed to stay below a high evaporation regime. It is also assumed this 2-D slice is positioned at the center of the trench, where TEMHD volume forces are lower than the trench boundaries. Inclusion of the high surface tension of liquid lithium plays a key role in maintaining a stable surface and is expected to help balance the increased volume forces near the trench edges. Inclusion of stronger TEMHD drive near the trench boundaries is expected to drive quicker flow than is demonstrated here and improve reliability under high heat fluxes. These physics and their effects will be investigated in future work extending this modeling into full 3-D free surface fluid dynamics.

While the trench shaping shown here may have the ability to reduce the risk of dryout, experimentally the solution is limited in scope due to the precision required in the design. The ledge placement must be accurate to within $1-3$ cm, or the liquid response from the step height will not be impacted by the highest heat flux and dryout could occur. In large scale devices, any shift in plasma configuration would lessen the

effectiveness of this trench shaping, and transient events elsewhere on the wall cannot be predicted and therefore cannot be protected against. Thus, geometries with a more inherent resistance to dryout must be explored. Future work will examine advanced geometries to find a more general solution.

The 2-D dryout model does provide insight into potential mitigation strategies, and future work will attempt to extend the model to full 3-dimensional implementation. To accomplish this goal, issues with the solid-liquid interface conditions must be addressed. Better diagnostic preparation coupled with further testing of dryout solutions will also allow stronger quantitative analyses of dryout parameters for refinement of the models. Information from these tests will be used to update future versions of dryout models, which will be able to predict more than the transient conditions, and instead provide information on steady state flow based on the geometries tested. In this way, faster iteration of design proposals can be achieved, and the solutions implemented will bring LiMIT closer to demonstrating full viability in fusion-relevant conditions.

Acknowledgements

This work was supported by Department of Energy/ALPS contract DE-FG02-99ER54515. The use of COMSOL Multiphysics is provided by the Beckman Institute Visualization Laboratory at the University of Illinois at Urbana-Champaign.

References

[1] G. Federici, H. Wuerz, G. Janeschitz, R. Tivey, Erosion of plasma-facing components in ITER, Fusion Eng. Des. 61-62 (2002) 81–94.
[2] A. Hassanein, Prediction of material erosion and lifetime during major plasma instabilities in tokamak devices, Fusion Eng. Des. 60 (2002) 527–546.
[3] G. Federici, et al., Effects of ELMs and disruptions on ITER divertor armour materials, J. Nucl. Mater. 337–339 (1–3) (2005) 684–690.
[4] J.W. Coenen, et al., Evolution of surface melt damage, its influence on plasma performance and prospects of recovery, J. Nucl. Mater. 438 (2013).
[5] M.J. Baldwin, R.P. Doerner, Formation of helium induced nanostructure 'fuzz' on various tungsten grades, J. Nucl. Mater. 404 (2010) 165–173.
[6] G.M. Wright, et al., Comparison of tungsten nano-tendrils grown in Alcator C-Mod and linear plasma devices, J. Nucl. Mater. 438 (2013) S84–S89.
[7] J. Wesson, Tokamaks, 4th ed., Oxford University Press, New York City, 2011.
[8] R. Majeski, et al., CDX-U operation with a large area liquid lithium limiter, J. Nucl. Mater. 313–316 (2003) 625–629.
[9] R. Majeski, et al., Recent liquid lithium limiter experiments in CDX-U, Nucl. Fusion 45 (6) (2005) 519–523.
[10] R. Majeski, et al., Enhanced energy confinement and performance in a low-recycling tokamak, Phys. Rev. Lett. 97 (7) (2006).
[11] A.A. Tuccillo, et al., Overview of the FTU results, Nucl. Fusion 49 (10) (2009).
[12] J.C. Schmitt, et al., High performance discharges in the Lithium Tokamak eXperiment with liquid lithium walls, Phys. Plasmas 22 (5) (2015).
[13] D.K. Mansfield, et al., Transition to ELM-free improved H-mode by lithium deposition on NSTX graphite divertor surfaces, J. Nucl. Mater. 390–391 (1) (2009) 764–767.
[14] L.R. Baylor, et al., High frequency ELM pacing by pellet injection on DIII-D and implications for ITER, 39th EPS Conference on Plasma Physics 2012, EPS 2012 and the 16th International Congress on Plasma Physics 1 (2012).
[15] M.G. Bell, et al., Plasma response to lithium-coated plasma-facing components in the National Spherical Torus Experiment, Plasma Phys. Control. Fusion 51 (2009) 12.
[16] R. Maingi, et al., The effect of progressively increasing lithium coatings on plasma discharge characteristics, transport, edge profiles and ELM stability in the National Spherical Torus Experiment, Nucl. Fusion 52 (8) (2012).
[17] H.W. Kugel, et al., NSTX plasma operation with a Liquid Lithium Divertor, Fusion Eng. Des. 87 (2012) 1724–1731.
[18] M.A. Jaworski, et al., Liquid lithium divertor characteristics and plasma-material interactions in NSTX high-performance plasmas, Nucl. Fusion 53 (August 8) (2013).
[19] D.N. Ruzic, W. Xu, D. Andruczyk, M.A. Jaworski, Lithium-metal infused trenches (LiMIT) for heat removal in fusion devices, Nucl. Fusion 51 (10) (2011).
[20] J.S. Hu, et al., First results of the use of a continuously flowing lithium limiter in high performance discharges in the EAST device, Nucl. Fusion 56 (4) (2016).
[21] G.Z. Zuo, et al., Mitigation of plasma-material interactions via passive Li efflux from the surface of a flowing liquid lithium limiter in EAST, Nucl. Fusion 57 (4) (2017).
[22] G.Z. Zuo, et al., Results from an improved flowing liquid lithium limiter with increased flow uniformity in high power plasmas in EAST, Nucl. Fusion 59 (1) (2019).
[23] J.A. Shercliff, Thermoelectric magnetohydrodynamics, J. Fluid Mech. 91 (2) (1979) 231–251.
[24] M.A. Jaworski, et al., Thermoelectric Magnetohydrodynamic Stirring of Liquid Metals, (2020).
[25] W. Xu, D. Curreli, D. Andruczyk, T. Mui, R. Switts, D.N. Ruzic, Heat transfer of TEMHD driven lithium flow in stainless steel trenches, J. Nucl. Mater. 438 (2013).
[26] W. Xu, D. Curreli, D.N. Ruzic, Computational studies of thermoelectric MHD driven liquid lithium flow in metal trenches, Fusion Eng. Des. 89 (12) (2014) 2868–2874.
[27] W. Xu, et al., Vertical flow in the thermoelectric liquid metal plasma facing structures (TELS) facility at Illinois, J. Nucl. Mater. 463 (2015) 1181–1185.
[28] J.S. Hu, et al., An overview of lithium experiments on HT-7 and EAST during 2012, Fusion Eng. Des. 89 (12) (2014) 2875–2885.
[29] G.Z. Zuo, et al., Liquid lithium surface control and its effect on plasma performance in the HT-7 tokamak, Fusion Eng. Des. 89 (12) (2014) 2845–2852.
[30] P. Fiflis, et al., Performance of the lithium metal infused trenches in the magnum PSI linear plasma simulator, Nucl. Fusion 55 (11) (2015).
[31] Z. Ma, Y. Nina, S. Qiu, W. Tian, G. Su, Application of Film Dryout Model in Liquid Metal CHF Prediction, (2014) p. V02AT09A023.
[32] W. Xu, Experimental and Numerical Analysis of Thermoelectric Magnetohydrodynamic Driven Liquid Lithium Flow in Open Channels for Fusion Applications, University of Illinois at Urbana-Champaign, 2015.
[33] COMSOL Multiphysics Reference Manual, Version 4.3, (2014).